Research Article

Panpan Sun, Shuzhong Wang*, Yanhui Li, Tuo Zhang, Dong Wang, Baoquan Zhang, Jianqiao Yang, and Donghai Xu

One-pot synthesis of nano titanium dioxide in supercritical water

https://doi.org/10.1515/ntrev-2020-0030
received October 20, 2019; accepted November 05, 2019

Abstract: Supercritical hydrothermal synthesis of nanosized metal oxides is of great interest for scholars due to its one-pot and readily realizing commercial production process. Hydrothermal synthesis of nanosized TiO_2 in subcritical and supercritical water was investigated with different reaction temperatures (250–450°C), time (3–10 min), precursor species ($Ti(SO_4)_2$, $TiCl_4$), and the addition of a surfactant ($CH_3(CH_2)_5NH_2$). TiO_2 synthesized under supercritical state has a higher degree of crystallinity when compared with TiO_2 obtained from subcritical state, which is attributed to a higher reaction rate. Extending reaction time from 3 to 10 min leads to the growth of crystal and broader size distribution (36.66 ± 8.5 nm). More uniform products can be obtained when $Ti(SO_4)_2$ acting as the precursor compared with $TiCl_4$ being the precursor. The application of surfactant $CH_3(CH_2)_5NH_2$ in the synthesis makes chemical bonding between the particle surface and organic ligand. It affects the growth direction of TiO_2 crystal; as a result, rod-like TiO_2 crystal is obtained.

Keywords: supercritical water, nanoparticles, titanium dioxide

1 Introduction

Nanoscale titanium dioxide (TiO_2) is a new type semiconductor inorganic material with diverse applications, such as photocatalysts [1], lithium batteries [2], wasted water treatment processes [3], and dye-sensitized solar cells [4]. These are attributed to its unique properties such as photocatalytic function, better thermal and chemical stability, strong absorbing UV ability, nontoxicity, and self-cleaning function [5,6]. It is well known that materials appear to possess unique properties while one or more than one of their three dimensions is in nanoscale (1–100 nm). This means that the size and morphology of nanomaterials play crucial roles in the performance during their applications. In general terms, it is the synthesis method that determines the fundamental characteristics of nanomaterials, which, accordingly, are of great importance in the subsequent practical applications. As for nanosized TiO_2, they have been synthesized with a broad range of methods, including sol–gel method [7], reverse micelles reaction [8], gas-phase synthesis [9], sonochemical synthesis [10], and hydrothermal technique [11]. Sol–gel method is used widely, but not suitable for large-scale commercial production because of its costly process. As for reverse micelles reactions, a rather long time (several tens of days) is usually needed to get mature products. On the other hand, products obtained from reverse micelles reactions are usually amorphous because the reaction is conducted at the low-reaction temperature, usually at room temperature [12]. Gas-phase synthesis allows excellent control of size and dispersity, however limited by its precise equipment requirement [13]. Sonochemical synthesis is an energy-efficient and simple process, but powder synthesized in this way usually needs further treatment, i.e., calcination [14], which makes sonochemical synthesis less desirable than the one-step synthesis process. Comparing with the mentioned fabrication pathways, the hydrothermal technique is a nanomaterial synthesis method with the benefit of being cheap, gentle, simple, and easily scalable.

Supercritical water ($T > 373.9$°C, $P > 22.1$ MPa) is a unique solvent, in which negative solubility materials have an extremely low solubility due to the low dielectric constant of water in supercritical conditions [15]. This is exactly the theory applied in supercritical hydrothermal synthesis. Besides this, various fluid properties have an intriguing change, such as density of molecules, thermal conductivity,

* **Corresponding author: Shuzhong Wang,** Key Laboratory of Thermo-Fluid Science and Engineering, Ministry of Education, Department of Thermal Engineering, School of Energy and Power Engineering, Xi'an Jiaotong University, Xi'an, Shaanxi, 710049, China, e-mail: szwang@aliyun.com
Panpan Sun, Yanhui Li, Tuo Zhang, Dong Wang, Baoquan Zhang, Jianqiao Yang, Donghai Xu: Key Laboratory of Thermo-Fluid Science and Engineering, Ministry of Education, Department of Thermal Engineering, School of Energy and Power Engineering, Xi'an Jiaotong University, Xi'an, Shaanxi, 710049, China

and diffusion coefficient. These changes contribute to supercritical hydrothermal synthesis (SHS), making it more efficient than the normal hydrothermal synthesis method, let alone the nature of environmentally benign [16]. During the past two decades, various metal oxides and zero-valent metal particles were synthesized by taking advantage of the SHS method, including ZnO [17], CuO [18], Co_3O_4 [19], $LiFePO_4$ [20], TiO_2 [21–28], Ag [29], Cu [30], and Ni [31]. Tadafumi Adschiri et al. [21] reported a first try of synthesizing anatase TiO_2 using the supercritical hydrothermal synthesis technology (30 MPa and 400–450°C) in 1992, which is attracting extensive attention from other scholars. Tahereh Mousavand et al. [22] synthesized TiO_2 nanoparticles from supercritical hydrothermal synthesis with the addition of organic modifier ($CH_3(CH_2)_4CHO$); the dispersive property of obtained TiO_2 was detected. They found that TiO_2 nanoparticles have a good dispersity in the organic solvent. These researches are not comprehensive, and it is hard for us to extract full view of synthesizing TiO_2 in supercritical water. Eltzholtz et al. [23] studied the influence of reaction temperature (300–550°C) and residence time (0–500 s) on crystallite size of nano titania in supercritical water–isopropanol mixture reaction conditions, and direct observation was got with the contribution of *in situ* synchrotron investigations combined with a new pulsed supercritical synthesis method. Neel M. Makwana et al. [24] studied the effect of reaction pH on average crystallite size of nano titania at a set reaction temperature (305°C). Jian-Li Mi et al. [25] observed phase transformation from broolite and anatase to rutile TiO_2 during the reaction of 20 min at a rather low reaction temperature (300°C). Jian-Li Mi et al. [26] studied on continuous flow supercritical synthesizing anatase-TiO_2 nanocrystals. Shin-Ichiro Kawasaki et al. [27] synthesized TiO_2 nanoparticles using a continuous supercritical hydrothermal synthesis method, in which $Ti(SO_4)_2$ is used as a precursor and KOH is added. Hiromichi Hayashi et al. [28] made research on synthesizing nano titania with subcritical and supercritical water (200–400°C) for a long time duration (2–24 h) using batch reactors. As we all know, the key part of the SHS method is the rapid heating of the precursor. Different heating method and heating rate result in different crystal formation and growth mechanism. The general heating rate sequence is continuous flow reactor > batch reactor (smaller volume) > batch reactor (bigger volume). It is meaningful to have a comprehensive study and deep understanding of parameter effect in one kind of heating rates. Also, to make a contribution to Green Earth, pure water was used as solvent without organics. In the present work, the effects of operation parameters (temperature, reaction time, precursor species, surface modification) on TiO_2 nanocrystallite characteristics are discussed, during which water is used as a sole solvent. Hexylamine is a commonly used organic surfactant in SHS [32]; however, the effect of hexylamine on TiO_2 crystal formation has not been studied. In this work, the effect of hexylamine on nano TiO_2 morphology is studied. At last, an innovative nano TiO_2 formation mechanism with the existence of surfactants was proposed.

2 Materials and methods

2.1 Materials and procedures

Titanium(IV) sulfate ($Ti(SO_4)_2$, purity > 97.0 wt%), titanium(IV) chloride ($TiCl_4$, purity > 99.0 wt%), and ethanol were purchased from Sinopharm Chemical Reagent Co., Ltd (Shanghai, China). Potassium hydroxide (KOH, purity > 99.0 wt%) and hexylamine ($CH_3(CH_2)_5NH_2$, purity > 99.0 wt %) were purchased from Sigma Aldrich (Shanghai, China). All reagents were used as received without further purification. Distilled and deionized (DDI) water was used to prepare a metal salt aqueous solution. High-pressure tube reactors were made of stainless steel 316 and have an inner volume of 5.8 mL (inner diameter and length of 8.7 and 90.0 mm, respectively). A predetermined amount of prepared titanium salt aqueous solution was loaded into reactors; afterward, tube reactors were sealed with plugs combined with cutting sleeves. The predetermined amount of prepared titanium salt aqueous solution was calculated depending on water density at the desired temperature to obtain a spontaneous specific pressure within the enclosure space. The sealed tube reactors were subsequently immersed into a fluidized sand bath for definite reaction time. The fluidized sand bath was preheated electrically and maintained at a pre-set temperature. Then, the reactions in tube reactors were terminated by quenching the tube reactors in a cold-water bath. The solid phase products and liquid phase effluent were separately exported from reactors and transferred into centrifuge tubes. Solid products were purified by repeating decantation and centrifugation in ethanol or DDI water several times. Finally, the white-color powder was obtained after vacuum drying solid products for 24 h at 105°C.

2.2 Analysis means

The titanium ions remained in the liquid phase effluent after the reaction was evaluated by inductively coupled

plasma emission spectroscopy (Shimadzu, ICPE-9000, Japan). The percent conversation (%) of titanium ions in the reaction was calculated by using the following equation:

$$\alpha = \frac{[Ti^{4+}]_0 - [Ti^{4+}]_1}{[Ti^{4+}]_0} \times 100\%$$

in which α is percent conversion of titanium ions, $[Ti^{4+}]_0$ is the initial concentration of titanium ions in the precursor, and $[Ti^{4+}]_1$ is the concentration of titanium ions in liquid phase effluent after the reaction.

The solid products were analyzed by X-ray diffractometry (XRD), transmission electron microscopy (TEM), and Fourier transform infrared spectroscopy (FT-IR). The XRD data were measured on an X'pert Pro diffractometer (Rigaku, D/MAX-2400, Netherlands) with Cu Kα irradiation. The preparation procedure of TEM (JEM-2100, Japan) samples is ultrasonic dispersion nanoparticles into ethanol and make sure that they are mixed uniform, adding droplets of the dispersed powder on a copper grid. TEM images were used to identify the size and morphology of synthesized products. FT-IR spectra were measured to analyze the chemical bonding between the organic modifier and particle surface with a Fourier transformed infrared spectrometer (Bruker, TENSOR 27, Germany). The crystallite size was calculated based on the Scherrer equation:

$$D = \frac{K\lambda}{\beta \cos\theta}$$

in which D represents the crystallite size, K is the Scherrer constant, $K = 0.89$; λ represents the wavelength of X-ray, $\lambda = 0.154056$ nm; β is the full width at half maximum (FWHM) of X-ray diffraction; θ represents the Bragg angle. FWHM was extracted from X-ray diffraction measurement and the broadening caused by the instrument was eliminated.

3 Results and discussion

3.1 Effects of temperature

To explore the role of temperature in SHS of TiO_2 nanoparticles, experiments were taken at different temperatures (250–500°C) with an interval of 50°C. The concentration of precursor ($Ti(SO_4)_2$) was set to be 0.04 mol/L and a calculated amount of KOH was added, resulting in a concentration of 0.16 mol/L. The reaction time is 3 min, including the heating time. The XRD results are shown in Figure 1, which demonstrates that products belong to anatase (PDF#21-1272). From the evolution of XRD data obtained at different temperatures, we can see that the diffraction peaks become more sharply and narrower with increasing temperatures. This evolution trend indicates that higher reaction temperature facilities the formation of higher crystallinity products. The difference of crystallinity is also confirmed by selected area electron diffraction measurement in the later part; the detailed explanation can be found in the next paragraph.

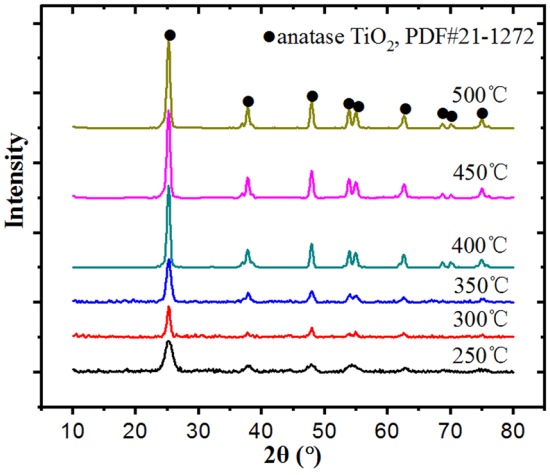

Figure 1: XRD results of products synthesized at different temperatures and 30 MPa.

The morphology and size of TiO_2 crystals were changed by the adjustment of reaction temperature, as demonstrated in Figure 2. This figure shows the TEM pictures of TiO_2 products synthesized at 300, 400, and 500°C. TEM pictures collected from products synthesized at 250, 350, and 450°C can be found in the supporting information. At the subcritical region, the synthesized nanoparticles are spherical with blurry boundary, which is another evidence for low crystallinity. However, at the supercritical region, rhombic and rectangle nanocrystals with clear boundaries are synthesized. This change demonstrates that high-temperature facilities the formation of a high degree of crystallinity crystals. The particle size of TiO_2 synthesized at different temperatures was measured by hand, and the column diagrams are shown in Figure 3. For these polygon crystals, the length of width and length were all measured to represent the size, the size distributions were statistic results without distinguishing the width and length. The size distribution

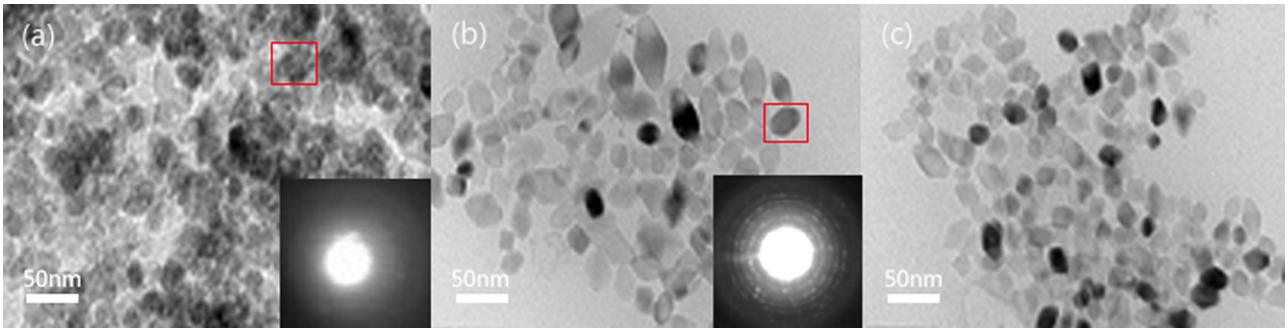

Figure 2: TEM pictures of TiO_2 synthesized at 30 MPa and different temperatures (a) 300°C, right corner – SAED picture obtained from red frame (b) 400°C, right corner – SAED picture obtained from red frame (c) 500°C as 0.04 M $Ti(SO_4)_2$ being precursor and 0.16 M KOH was added.

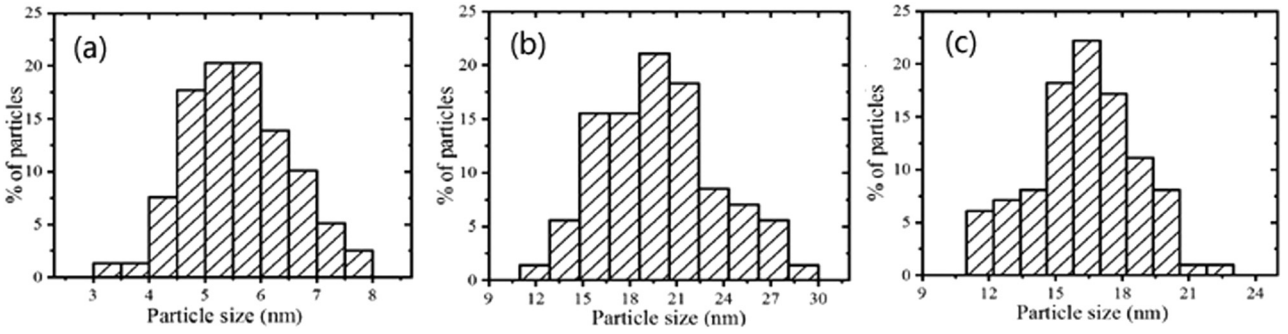

Figure 3: Size distribution of products synthesized at (a) 300°C (b) 400°C (c) 500°C and 30 MPa when $Ti(SO_4)_2$ acted as a precursor and 0.16 M KOH was added.

collected from 250, 350, and 450°C samples can be found in the supporting information. The average sizes of products collected at 250, 300, 350, 400, 450, and 500°C were 5.6, 6.8, 8.8, 19.8, 18.9, and 18.8 nm separately. With the increasing reaction temperature, the particle size increased; however, no big difference happened once the reaction temperature is higher than the critical point (400, 450, and 500°C). A significant increase in size was observed when the reaction temperature increased to the supercritical region (from 350 to 400°C). On the one hand, due to the extremely low dielectric constant of water in the supercritical region, a low solubility of intermediate products and metallic oxide was obtained. On the other hand, depending on the Born-type equation [33], the reaction rate is inversely proportional to dielectric constant, thus extremely low dielectric constant leads to fast hydrolysis, dehydration, and nucleation rate compared to them at the subcritical region. These can explain the formation of high crystallinity products. To explain the evolution of average size, selected area electron diffraction (SAED) was applied on products (labeled by the red frame in TEM pictures) obtained at 300 and 400 °C. The SAED results are shown in the right corner of Figure 2a and c. The SAED pictures demonstrate that products obtained at the subcritical region was nearly amorphous or products with quite low crystallinity; however, TiO_2 synthesized at 400°C was polycrystal. This may explain the increasing trend of average size from subcritical condition to supercritical condition, which should have an inverse trend for crystals.

3.2 Effects of reaction time

The effects of reaction time were explored while 0.04 M $Ti(SO_4)_2$ acting as a copper source with the addition of 0.16 M KOH. The reaction temperature and pressure were maintained at 400°C and 30 MPa, separately. Three different reaction times were explored in this work, they are 3, 5, and 10 min, respectively. The X-ray diffraction results indicate that all the products are anatase TiO_2, see PXRD spectrogram in the supporting information. The conversion of Ti^{4+} with time did not change much, from 99.13% (3 min) to 99.21% (10 min), indicating the very fast hydrolysis and dehydration reaction rates at the supercritical condition. The corresponding crystallite

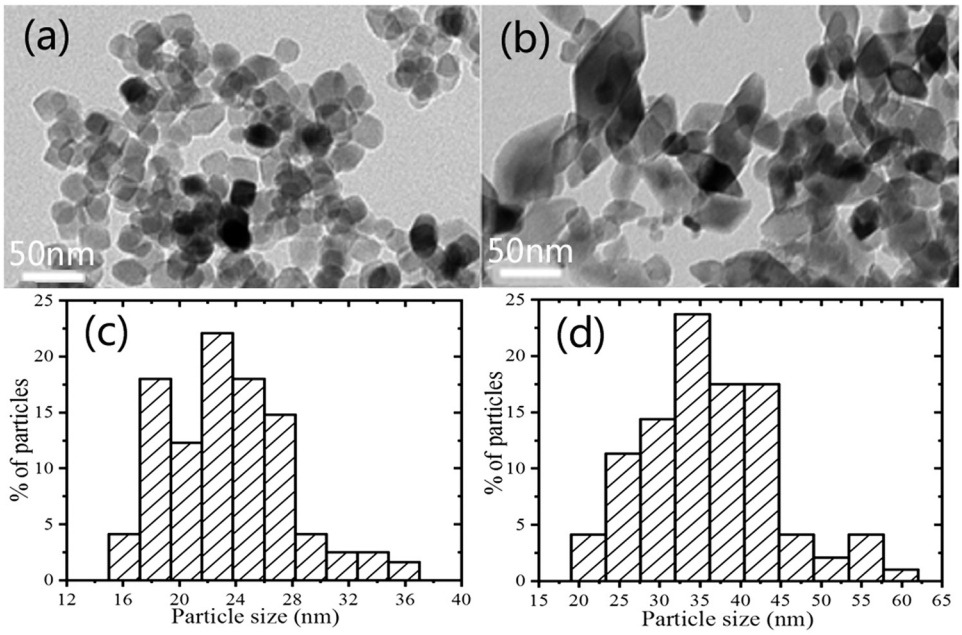

Figure 4: TEM pictures of TiO_2 synthesized at 30 MPa and different times (a) 5 min (b) 10 min and their corresponding size distribution (c) 5 min (d) 10 min as 0.04 M $Ti(SO_4)_2$ being precursor and 0.16 M KOH was added.

size of products calculated from PXRD is 16.97, 17.20, and 16.53 nm for the reaction time of 3, 5, and 10 min. There is not a significant change in crystallite size when changing reaction time from 3 to 10 min. However, the extension of reaction time resulted in an increase and broaden of particle size, as shown in Figure 4. The average particle size of TiO_2 synthesized after 10 min is 36.66 ± 8.5 nm. Indicating that longer reaction time does not benefit the formation of uniform and smaller crystal. Another meaningful point is the morphology change, the product collected after 10 min is aggregation with irregular shape and no clear border. The long

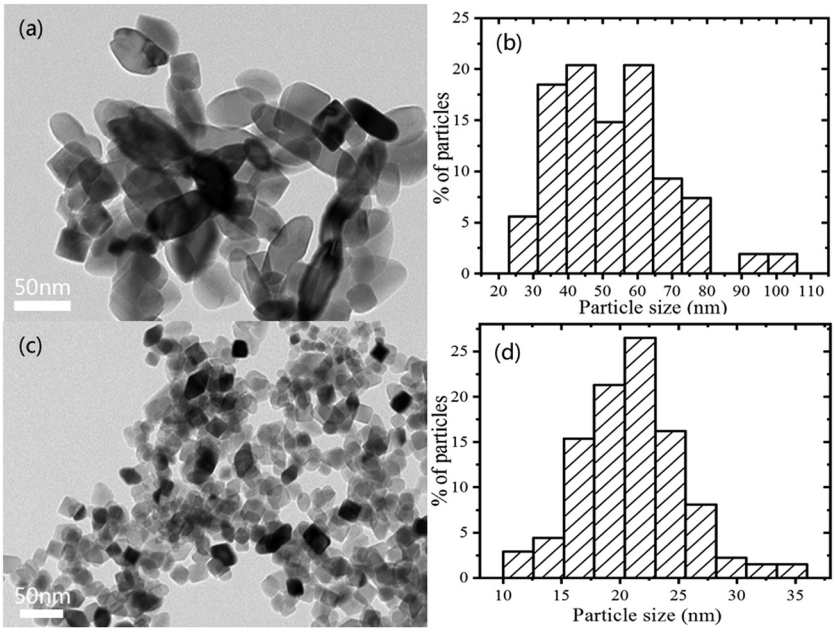

Figure 5: TEM photographs and size distributions of products collected from $TiCl_4$ at 400°C and 30 MPa, (a) and (b) $[OH]^-/Ti^{4+} = 4$, (c) and (d) $[OH]^-/Ti^{4+} = 5$.

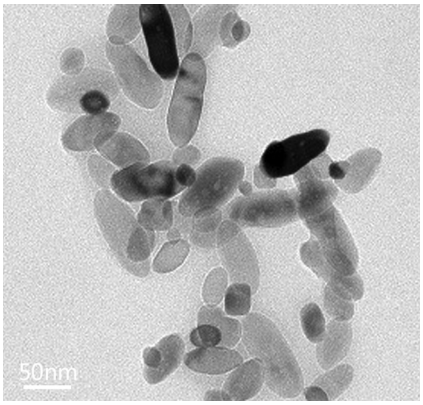

Figure 6: TEM pictures of products synthesized with hexylamine with $Ti(SO_4)_2$ as a titanium source.

high-temperature condition may result in the aggregation of smaller crystals to decrease the surface energy and make the reaction system more stable.

3.3 Effects of precursor species

$TiCl_4$ was chosen as a different titanium source to explore the effect of precursor species through comparing with results from $Ti(SO_4)_2$. The concentration of $TiCl_4$ was set at 0.04 M, and 0.16 M KOH was added to facilitate the hydrolysis. The reaction temperature, pressure, and time were 400°C, 30 MPa, and 3 min, respectively. PXRD detection of products from $TiCl_4$ shows that products are anatase TiO_2, and the corresponding PXRD data can be found in the supporting information. The TEM photograph of products and the corresponding size distribution are shown in Figure 5a and b. The average particle size is 52 nm with a broad range. The difference between the two kinds of precursor solution is the pH value. The pH of $Ti(SO_4)_2$ is about 7 with the addition of 0.16 M KOH; however, the pH of $TiCl_4$ is about 2 with the addition of 0.16 M KOH. At acid condition, the solubility of TiO_2 is high, then resulting in low supersaturation, which leads to bigger particle size due to the consumption of Ti^{4+} in growth rather than in new nuclei formation. To verify this theory, another experiment point with 0.2 M KOH was made. The TEM photograph and corresponding size distribution are shown in Figure 5c and d. The average particle size is 21 nm with a narrow range.

3.4 Surface modification with surfactant

Hexylamine ($CH_3(CH_2)_5NH_2$) was used as a surfactant to explore the surface modification of TiO_2 nanoparticles. 0.04 M $Ti(SO_4)_2$ was used as a titanium source and 0.16 M KOH was added. The reaction temperature, pressure, and time were 400°C, 30 MPa, and 3 min, respectively. TEM pictures of obtained products are shown in Figure 6. We can see from the pictures, the morphology of TiO_2 synthesized with hexylamine is rod-like. To check the surface properties of TiO_2, their dispersibility was examined by putting the particle products in a binary solvent system of water and trichloromethane. The products without organic-modified were dispersed in the water phase, as shown in Figure 7a. The hexylamine-modified particles were

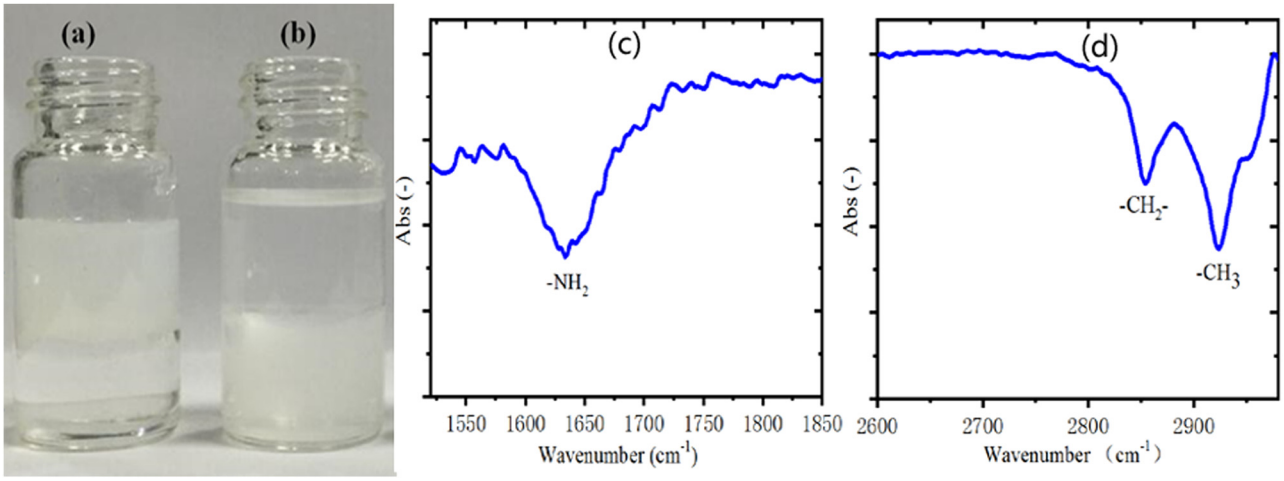

Figure 7: Dispersibility of TiO_2 nanoparticles synthesized (a) in the absence of organic reagent and (b) in the presence of $CH_3(CH_2)_5NH_2$ and FT-IR spectra of TiO_2 nanoparticles synthesized with $CH_3(CH_2)_5NH_2$.

dispersed in the trichloromethane phase, as shown in Figure 7b. These results indicate that the surface of TiO_2 was covered with organic ligands.

To further investigate the surface nature and chemical bonding between the surface of nanocrystals and organic molecules, Fourier transform infrared (FT-IR) analysis was carried out. The FT-IR spectra of TiO_2 nanoparticles synthesized with hexylamine are shown in Figure 7c and d. We can see from the figure that two bands appear at 2,924 and 2,854 cm^{-1}, which corresponding to the stretching mode of methyl and methylene groups. Also, $-NH_2$ group is observed at 1,634 cm^{-1}. These suggest that the organic ligand was chemically bonded to the surface of TiO_2 nanocrystals. The formation of rod-like TiO_2 is because the monamine organic ligand is ready to attach to a lattice plane and leads to the growth in one direction [34]. The morphology of nanosized TiO_2 is decided by the competitive growth between [101] and [001] directions [35,36]. The addition of hexylamine may result in a strong bind between organic ligands and {001} faces. The growth scheme diagram is shown in Figure 8. The growth along [001] is forbidden due to the adhesion of hexylamine; however, the growth along [101] direction occurs progressively, resulting in the disappearance of {001} face.

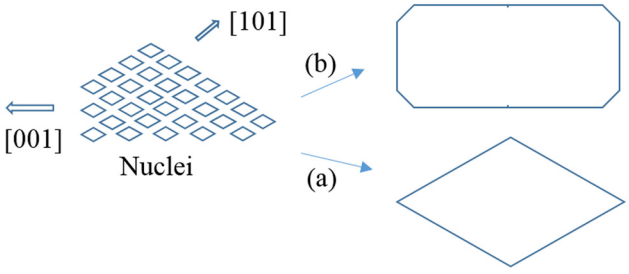

Figure 8: Scheme diagram of different morphology formation (a) without surfactant and (b) with $CH_3(CH_2)_5NH_2$.

4 Conclusion

A comprehensive research was made to explore the ability to synthesize TiO_2 nanoparticles taking advantage of supercritical water. Different influence factors including temperature, reaction time, precursor species, and surface modification with organic ligand were studied. Products synthesized at supercritical state have high crystallinity compared to them synthesized at subcritical conditions. Low reaction time (3 min) facilities the formation of small (19.8 nm) and narrow size distribution. Due to the hydrolysis properties of $TiCl_4$, it is not easy to form a uniform and small TiO_2 nanoparticles when compared with $Ti(SO_4)_2$. The surface nature properties and morphology of nanoparticles can be modified by adding organic ligand. Rod-like TiO_2 was obtained with the addition of hexylamine.

Acknowledgments: The authors are grateful for the support from the National Key Research and Development Program of China (2016YFC0801904), the Fundamental Research Funds for the Central Universities (xjj2018006) and (xjj2018201), and the Projects from National Natural Science Foundation of China (51871179).

Conflict of interest: The authors declare no conflict of interest regarding the publication of this paper.

References

[1] Xue C, Zhang TX, Ding SJ, Wei JJ, Yang GD. Anchoring tailored low-index faceted BiOBr nanoplates onto TiO_2 nanorods to enhance the stability and visible-light-driven catalytic activity. ACS Appl Mater Interfaces. 2017;9:16091–102.
[2] Wagemaker M, van de Krol R, Kentgens APM, van Well AA, Mulder FM. Two phase morphology limits lithium diffusion in TiO_2 (anatase): a Li-7 MAS NMR study. J Am Chem Soc. 2001;123:11454–61.
[3] Fukahori S, Ichiura H, Kitaoka T, Tanaka H. Photocatalytic decomposition of bisphenol A in water using composite TiO_2–zeolite sheets prepared by a papermaking technique. Environ Sci Technol. 2003;37:1048–51.
[4] Hagfeldt A, Gratzel M. Molecular photovoltaics. Acc Chem Res. 2000;33:269–77.
[5] Dahl M, Liu Y, Yin Y. Composite titanium dioxide nanomaterials. Chem Rev. 2014;114:9853.
[6] Chen X, Selloni A. Introduction: titanium dioxide (TiO_2) nanomaterials. Chem Rev. 2014;114:9281.
[7] Joo J, Kwon SG, Yu T, Cho M, Lee J, Yoon J, et al. Large-scale synthesis of TiO_2 nanorods via nonhydrolytic sol–gel ester elimination reaction and their application to photocatalytic inactivation of E. coli. J Phys Chem B. 2005;109:15297–302.
[8] Lin J, Lin Y, Liu P, Meziani MJ, Allard LF, Sun YP. Hot-fluid annealing for crystalline titanium dioxide nanoparticles in stable suspension. J Am Chem Soc. 2002;124:11514–8.
[9] Chin S, Park E, Kim M, Bae GN, Jurng J. Synthesis and photocatalytic activity of TiO_2 nanoparticles prepared by chemical vapor condensation method with different precursor concentration and residence time. J Colloid Interface Sci. 2011;362:470–6.
[10] Zhu YC, Li HL, Koltypin Y, Hacohen YR, Gedanken A. Sonochemical synthesis of titania whiskers and nanotubes. Chem Commun. 2001;2616–7.
[11] Kartini I, Menzies D, Blake D, da Costa JCD, Meredith P, Riches JD, et al. Hydrothermal seeded synthesis of mesoporous titania for application in dye-sensitised solar cells (DSSCs). J Mater Chem. 2004;14:2917–21.
[12] Zhang DB, Qi LM, Ma JM, Cheng HM. Formation of crystalline nanosized titania in reverse micelles at room temperature. J Mater Chem. 2002;12:3677–80.

[13] Cargnello M, Gordon TR, Murray CB. Solution-phase synthesis of titanium dioxide nanoparticles and nanocrystals. Chem Rev. 2014;114:9319–45.
[14] Yu JC, Zhang LZ, Yu JG. Direct sonochemical preparation and characterization of highly active mesoporous TiO_2 with a bicrystalline framework. Chem Mater. 2002;14:4647–53.
[15] Adschiri T, Lee YW, Goto M, Takami S. Green materials synthesis with supercritical water. Green Chem. 2011;13:1380–90.
[16] Namratha K, Byrappa K. Novel solution routes of synthesis of metal oxide and hybrid metal oxide nanocrystals. Prog Cryst Growth Charact. 2012;58:14–42.
[17] Sue K, Murata K, Kimura K, Arai K. Continuous synthesis of zinc oxide nanoparticles in supercritical water. Green Chem. 2003;5:659–62.
[18] Sun PP, Wang SZ, Zhang T, Li YH, Guo Y. Supercritical hydrothermal synthesis of submicrometer copper(II) oxide: effect of reaction conditions. Ind Eng Chem Res. 2017;56:6286–94.
[19] Hao YL, Teja AS. Continuous hydrothermal crystallization of alpha-Fe_2O_3 and Co_3O_4 nanoparticles. J Mater Res. 2003;18:415–22.
[20] Hong SA, Kim SJ, Chung KY, Chun MS, Lee BG, Kim J. Continuous synthesis of lithium iron phosphate ($LiFePO_4$) nanoparticles in supercritical water: effect of mixing tee. J Supercritical Fluids. 2013;73:70–9.
[21] Adschiri T, Kanazawa K, Arai K. Rapid and continuous hydrothermal crystallization of metal–oxide particles in supercritical water. J Am Ceram Soc. 1992;75:1019–22.
[22] Mousavand T, Zhang J, Ohara S, Umetsu M, Naka T, Adschiri T. Organic-ligand-assisted supercritical hydrothermal synthesis of titanium oxide nanocrystals leading to perfectly dispersed titanium oxide nanoparticle in organic phase. J Nanopart Res. 2007;9:1067–71.
[23] Eltzholtz JR, Tyrsted C, Jensen KMO, Bremholm M, Christensen M, Becker-Christensen J, et al. Pulsed supercritical synthesis of anatase TiO_2 nanoparticles in a water–isopropanol mixture studied by in situ powder X-ray diffraction. Nanoscale. 2013;5:2372–8.
[24] Makwana NM, Tighe CJ, Gruar RI, McMillan PF, Darr JA. Pilot plant scale continuous hydrothermal synthesis of nano-titania; effect of size on photocatalytic activity. Mater Sci Semicond Proc. 2016;42:131–7.
[25] Mi JL, Clausen C, Bremholm M, Lock N, Jensen KMO, Christensen M, et al. Rapid hydrothermal preparation of rutile TiO_2 nanoparticles by simultaneous transformation of primary Brookite and anatase: an in situ synchrotron PXRD study. Cryst Growth Des. 2012;12:6092–7.
[26] Mi JL, Johnsen S, Clausen C, Hald P, Lock N, So L, et al. Highly controlled crystallite size and crystallinity of pure and iron-doped anatase–TiO_2 nanocrystals by continuous flow supercritical synthesis. J Mater Res. 2013;28:333–9.
[27] Kawasaki S, Xiuyi Y, Sue K, Hakuta Y, Suzuki A, Arai K. Continuous supercritical hydrothermal synthesis of controlled size and highly crystalline anatase TiO_2 nanoparticles. J Supercritical Fluids. 2009;50:276–82.
[28] Hayashi H, Torii K. Hydrothermal synthesis of titania photocatalyst under subcritical and supercritical water conditions. J Mater Chem. 2002;12:3671–6.
[29] Aksomaityte G, Poliakoff M, Lester E. The production and formulation of silver nanoparticles using continuous hydrothermal synthesis. Chem Eng Sci. 2013;85:2–10.
[30] Sun P, Gjørup FH, Ahlburg JV, Mamakhel A, Wang S, Christensen M. In situ in-house powder X-ray diffraction study of zero-valent copper formation in supercritical methanol. Cryst Growth Des. 2019;19:2219–27.
[31] Sue K, Suzuki A, Hakuta Y, Hayashi H, Arai K, Takebayashi Y, et al. Hydrothermal-reduction synthesis of Ni nanoparticles by superrapid heating using a micromixer. Chem Lett. 2009;38:1018–9.
[32] Rangappa D, Ohara S, Umetsu M, Naka T, Adschiri T. Synthesis, characterization and organic modification of copper manganese oxide nanocrystals under supercritical water. J Supercritical Fluids. 2008;44:441–5.
[33] Amis ES, Hinton JF. Chapter 5 – Solvent influence on rates and mechanisms. In: Amis ES, Hinton JF, editors. Solvent effects on chemical phenomena. New York, America: Academic Press; 1973.
[34] Zhong Z, Ng V, Luo J, Teh SP, Teo J, Gedanken A. Manipulating the self-assembling process to obtain control over the morphologies of copper oxide in hydrothermal synthesis and creating pores in the oxide architecture. Langmuir. 2007;23:5971–7.
[35] Jun Y-w, Casula MF, Sim J-H, Kim SY, Cheon J, Alivisatos AP. Surfactant-assisted elimination of a high energy facet as a means of controlling the shapes of TiO_2 nanocrystals. J Am Chem Soc. 2003;125:15981–5.
[36] Penn RL, Banfield JF. Morphology development and crystal growth in nanocrystalline aggregates under hydrothermal conditions: insights from titania. Geochim Cosmochim Acta. 1999;63:1549–1557.